

## Fluid Inclusion Studies on Quartz Veinlets at the Yeylagh-e-Gharechi Porphyry Copper Deposit, Arasbaran Metallogenic Belt, Northwestern Iran

Behzad Hajalilou<sup>1,\*</sup>, Nasim hajalilou<sup>2</sup>

1- Department of Geology, Payam Noor University, Iran.

2- Department of Earth Sciences, Shahid Beheshti University, Tehran, Iran

\* Corresponding Author: n.hajalilouyebonab@mail.sbu.ac.ir

*Received: 31 December, 2017 / Accepted: 17 June 2018 / Published online: 20 June 2018*

### Abstract

Yeylagh-e-Gharechi porphyry copper deposit is located in the Arasbaran metallogenic belt at northwestern Iran, 25 kilometer of Ahar. Porphyry mineralization at the Yeylagh-e-Gharechi deposit occurred in post-Oligocene quartz monzonite and monzonite bodies which was hosted by Eocene volcanic rocks. Mineralization occurred as veins, veinlets and dissemination in hypogene zone. Supergene zone has been demolished by erosion agents. Four types of quartz veinlets are recognized based on mineralogy and relative temporal relationship .distinguished during the study of the deposit. Fluid inclusion studies on fluids trapped in quartz type I (potassic zone) vein and veinlets which were taken from drill core samples indicated a wide range of homogenization temperature in the veinlets from 190° to 520° with salinity of 20-60 wt% NaCl equivalent. Mineralizing fluids density at the deposit was 0.8-1.2 g/cm<sup>3</sup>. Fluid inclusion studies suggested that Yeylagh-e-Gharechi deposit is probably a porphyry copper deposit. This deposit has many similarity with other copper-gold porphyry deposit in Iran such as Sar Cheshmeh.

**Keywords:** Fluid inclusion; Porphyry copper deposit; Yeylagh-e-Gharechi, Arasbaran; Iran.

### 1- Introduction

The majority of porphyry deposits were developed as a result of subduction magmatism in syn-subduction and post-collisional tectonic settings (Cooke et al., 2005; Sillitoe, 2010). These deposits similar mineralization and alteration patterns throughout the world (Gustafson and Hunt, 1975; Beane and Bodnar, 1995; Seedorff et al., 2005). Porphyry deposits in Iran are distributed in four different zones including Arasbaran, Middle and south east (Kerman) part of Uromieh-Dokhtar volcano-plutonic, Kerman and Eastern Iran belts (Aghazadeh et al., 2015). Recent studies demonstrated that most of the porphyry deposits in Iran developed in Eocene to Miocene post-collisional settings in the four porphyry mineralization zones and belts (Aghazadeh et

al., 2015). It was suggested that porphyry deposits in Iran developed as a result of partial melting of metamorphosed mafic lower crust with a contribution of metasomatized lithospheric mantle in a post-collisional tectonic setting (Shafiei et al., 2009; Aghazadeh et al., 2015).

The Yeylagh-e-Gharechi porphyry copper deposit is located in the Arasbaran belt at northwestern Iran, at 46° 52' E longitude and 38° 40' N latitude coordinates, 10 km east of Sungun deposit and 25 km northwest of Ahar city (Fig. 1).

Many exploration activities have done that including geological mapping and drilling by Mehr Asl Company .The maximum depth is 430

m. The studies focus mainly on the fluid inclusion at Yeylagh-e-Gharechi deposit.

## 2- Regional geology

Arasbaran porphyry copper belt in the northwestern Iran bridges eastern and western parts of the Alpine-Himalayan metallogenic belt. The belt stretches northwestward to Gharabagh Mountains in Azerbaijan which finally ends in Armenia and Turkey, hosting numerous porphyry copper deposits (Moritz et al., 2013; Aghazadeh et al., 2015). The belt extends south and southeastward into Central Iran metallogenic belt. Arasbaran belt is 70-80 Km wide and 400 Km long, including cretaceous and eocene volcano-sedimentary rock units intruded by oligomiocene intrusions (Fig. 1). Very small outcrops of Pre-Cambrian and Paleozoic formations similar to Central Iran observed in the area indicates similar geological history during these times (Aghanabati, 2006). Pre-Mesozoic strata were underlain by

Cretaceous flysch-type deposits and continental shelf carbonates associated with mainly Cenozoic volcanic rocks in the belt. Magmatism that initiated in Late Cretaceous, continued with widespread activity during Cenozoic and Quaternary (Aghazadeh, 2009). Mainly upper Cretaceous and Paleocene submarine Calc-alkaline volcanic rocks show basic to acidic composition (Aghazadeh, 2009). Cenozoic to Quaternary volcanism constitutes of two major Eocene and late Miocene-Quaternary activity. Eocene volcanic rocks which show mainly basic to intermediate composition have shoshonitic affinity (Jamali et al., 2009), underlain by late Miocene volcano-sedimentary sequences. Late Miocene-Quaternary volcanic rocks are characterized by basic to felsic volcanic and as well as pyroclastic rocks with calc-alkaline to shoshonitic and ultra-potassic affinity (Aghazadeh, 2009). The latest magmatic event is represented by alkaline rocks showing within-plate geochemical signatures (Babakhani, 1990).

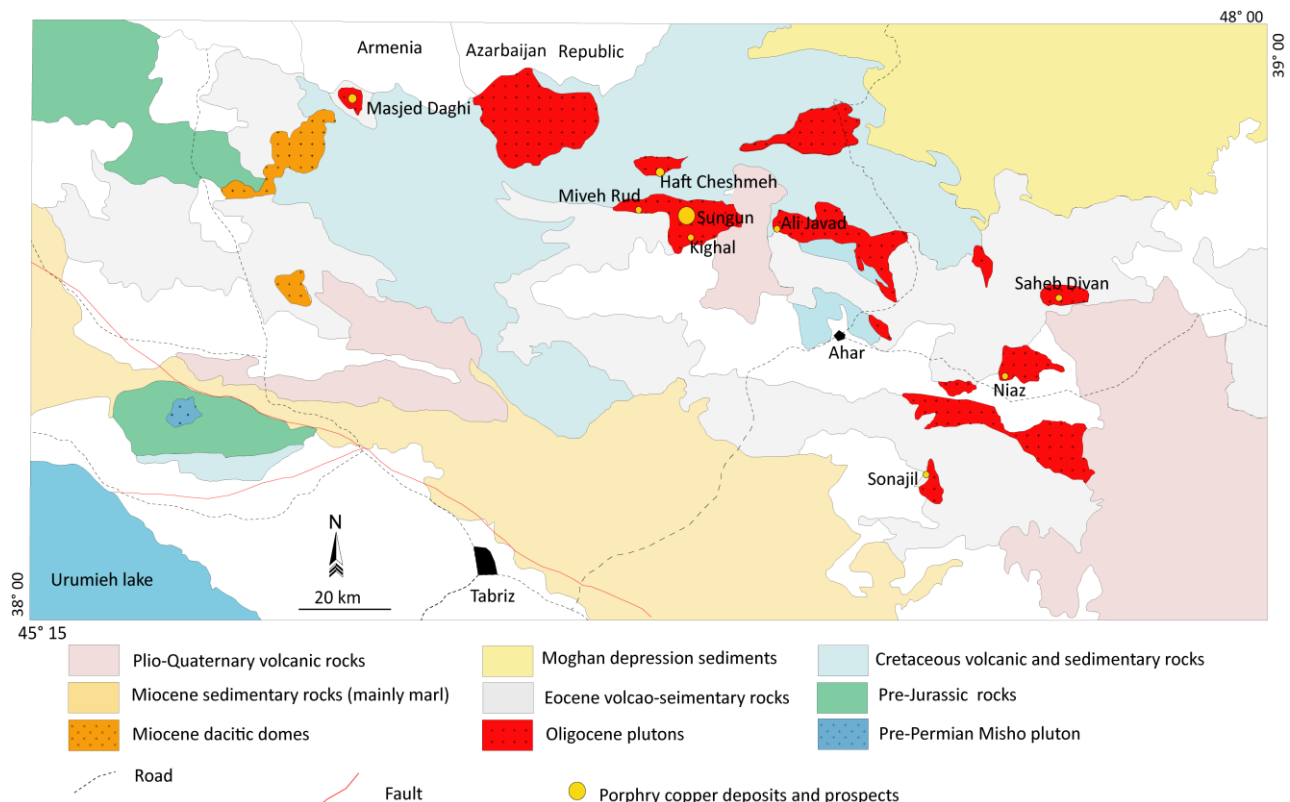


Figure 1) Geological map of Arasbaran belt and location of intrusive bodies as well as porphyry copper deposits (After Aghazadeh et al. 2015).

A wide variety of intrusive bodies of different nature and ages emplaced in the Arasbaran belt during Oligocene-Miocene (Babakhani et al., 1990; Jahangiri 2007; Aghazadeh et al., 2010, 2011; Castro et al., 2013). Extensive alteration zones as well as various mineralization such as porphyry, skarn and epithermal deposits have been developed throughout the belt during emplacement of Oligocene-Miocene intrusions (Mehrpartou 1993; Aghazadeh 2009; Jamali et al., 2009). In the Arasbaran belt, Plutonism initiated from middle to late Oligocene by calc-alkaline intrusion, followed by late Oligocene-lower Miocene shoshonitic intrusive bodies (Aghazadeh et al., 2011; Castro et al., 2013). Dacitic, granodioritic and monzonitic domes are the latest plutonic activity within the belt which cut through the earlier bodies. Shoshonitic intrusive bodies as well as younger domes are of adakitic nature while older intrusive bodies are of common calc-alkaline nature (Aghazadeh et al., 2011b). The formation of shoshonitic intrusions in the Arasbaran belt is attributed to partial melting of metasomatised lithospheric mantle in a post-collision tectonic setting (Aghazadeh et al. 2010, 2011; Castro et al., 2013) while younger adakitic intrusions are attributed to slab roll-back and melting of the subsiding slab (Jahangiri, 2007) and melting of lower mafic crust (Aghazadeh et al. 2015).

Porphyry copper mineralization in the Arasbaran belt is essentially associated with Oligo-Miocene intrusive bodies. More than ten deposits and prospects for porphyry copper deposits can be observed in the belt among which Sungun, MasjedDaghi, Haftcheshmeh, SahebDivan, Niyaz, MivehRude, Kighal, Alijavad and Yeylagh-e-Gharechi can be numerated (Fig. 1) where Sungun is considered as a world class deposit (Shafiei and et al., 2009). Based on the dating results made on the belt, porphyry copper deposits formed during two stages: late Oligocene (28-27 Ma) and early Miocene (22-20 Ma) (Aghazadeh et al., 2015). The formation of Yeylagh-e-Gharechi porphyry

copper deposit was attributed to younger plutonic activity in the area.

### 3- Geological setting and petrography

As mentioned earlier, Yeylagh-e-Gharechi porphyry copper deposit is located in Arasbaran belt. Outcrops in the belt are mainly of Tertiary age. Outcrops constitute of, Eocene volcanic and pyroclastic deposits as well as Oligo-Miocene intrusions which cut across earlier deposits. All these rock units were underlain by Plio-Quaternary volcanic and pyroclastic rocks (Fig. 2).

Oligo-Miocene granodioritic Shivar Dagh intruded in Eocene volcanic and pyroclastic deposits. Major outcrops at the periphery of the deposit are Eocene volcanic and pyroclastic deposits. Pyroclastic deposits constitute of tuff and lapilli tuff outcrops of andesitic composition which is likely the oldest outcrops within the deposit, the age of which is Eocene. Andesitic to trachy-andesitic outcrops cover the older units, which are host to the alteration and porphyry mineralization of the deposit (Hajalilou, 2016).

The youngest outcrops in the area are dacitic pyroclastic and basaltic volcanic rocks of Plio-Quaternary. These rocks cover vast areas in the western parts of the deposit. Several intrusions have been recognized at the deposit. The oldest intrusion at the deposit locality is Shivar Dagh quartz-diorite to granodiorite body with granular texture which show sometimes porphyroid texture (Hajalilou, 2016). Shivar Dagh is observed as E-W trending batholith where Yeylagh-e-Gharechi deposit is located at its westernmost part. The Shivar Dagh intrusion includes mainly amphibole and biotite and sometimes pyroxene as mafic minerals. Shivar Dagh intrusion show high-K calc-alkaline and adakitic nature which is emplaced in  $30.8 \pm 2.1$  Ma (Aghazadeh 2009; Aghazadeh et al., 2011).

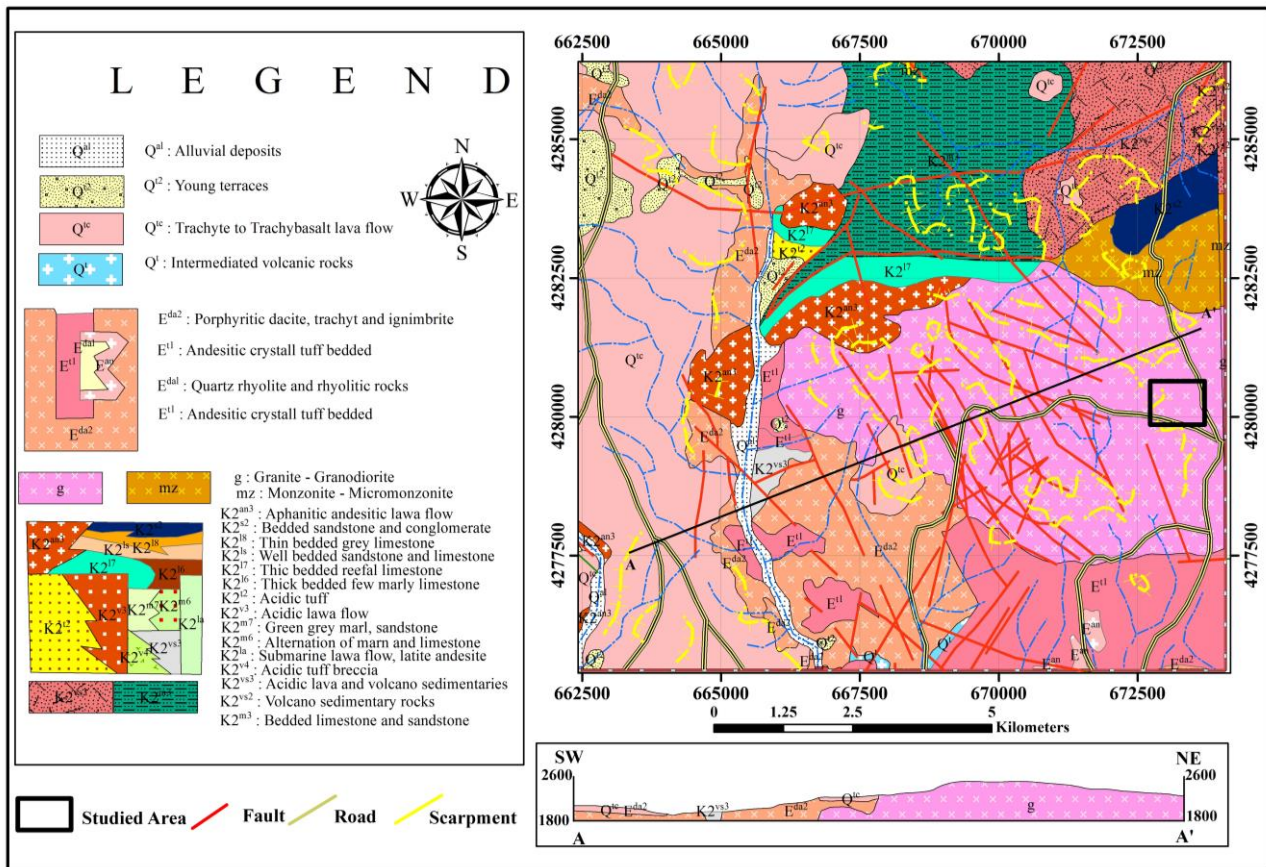


Figure 2) Geological map of Shivar Dagh and Yeylagh-e-Gharechi area (after Mehrparto, 1998).

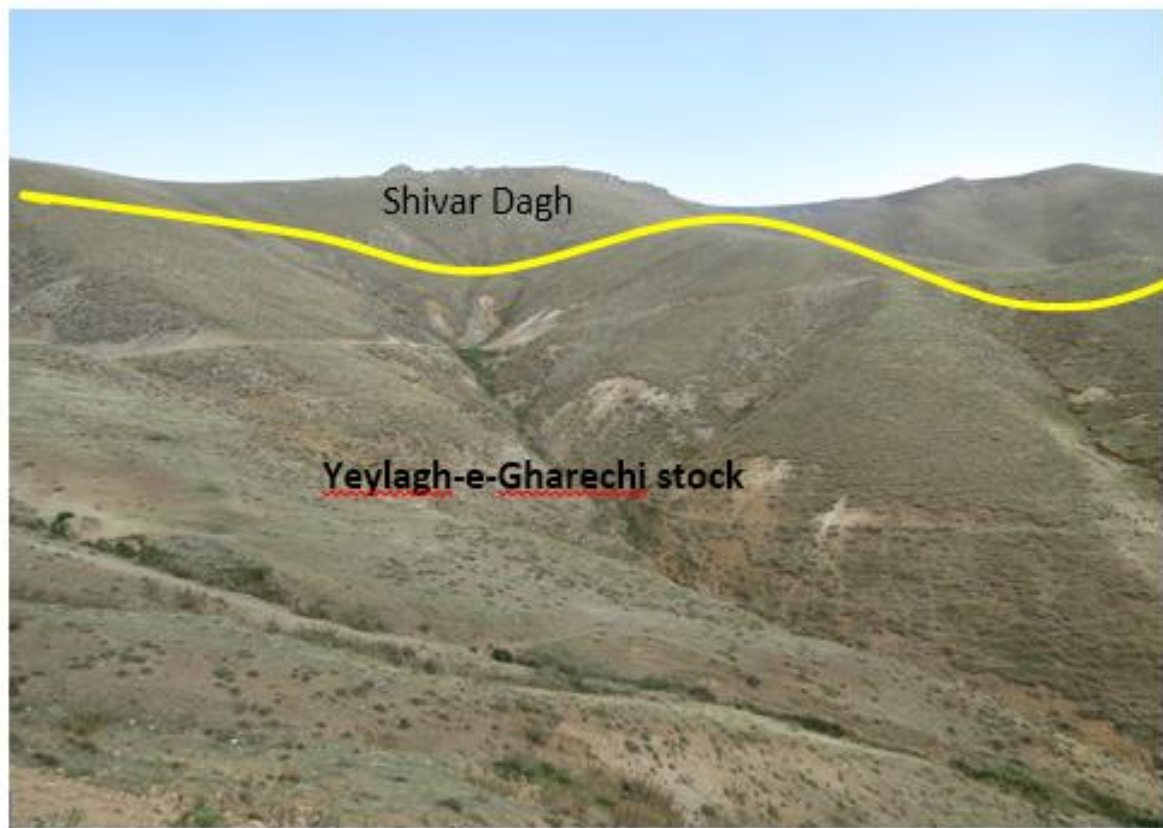


Figure 3) Shivar Dagh in Yeylagh-e-Gharechi area- Direction to north.

Yeylagh-e-Gharechi porphyry stock which is mineralizing agent for the porphyry deposit located at the central part of the deposit, is the associated with consequent alterations. The

porphyry body is 200m×450m, but the mineralization is mainly concentrated at the western part of the stock. The relationship between Yeylagh-e-Gharechi porphyry stock and the Shaivar Dagh granodioritic body is sometimes faulted, but it is likely that Yeylagh-e-Gharechi porphyry quartz monzonite is younger than Shaivar Dagh intrusion (Fig 3). The porphyry bodies are younger than

granitoid bodies (Hajalilou, 2016). Yeylagh-e-Gharechi porphyry body has porphyry texture with monzonitic to quartz monzonitic composition. Phenocrysts are mainly feldspars as well as mafic minerals such as biotite and amphibole (Fig 4). Development of different kind of alterations led to the replacement of primary minerals by secondary minerals.

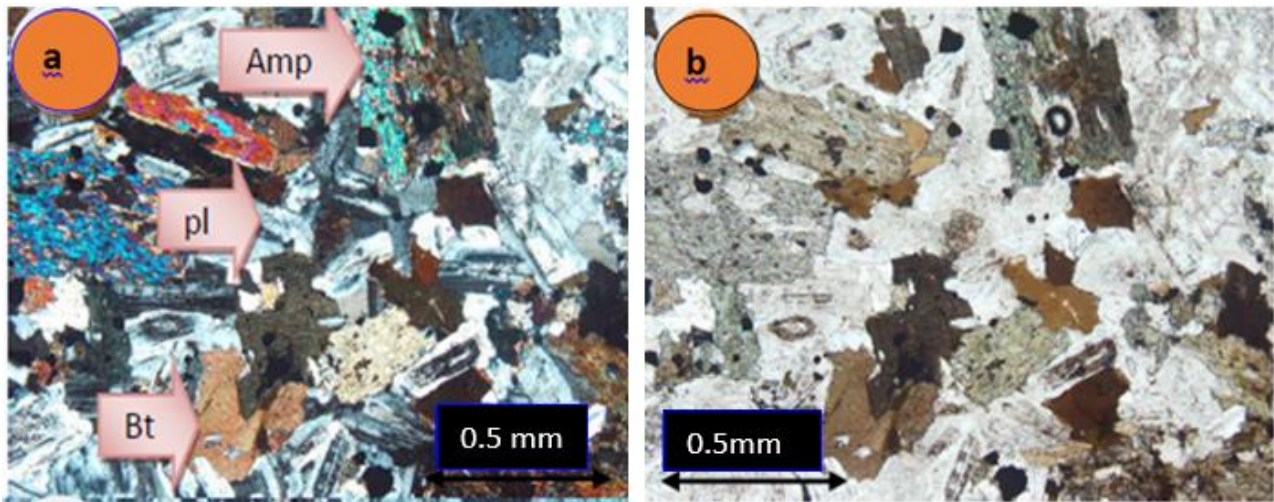


Figure 4) Plagioclase (pl), amphibole(Amp) and biotite (Bt) in monzonitic stock of Yeylagh-e-Gharechi A) xpl, B) ppl.

#### 4- Mineralization and alteration

Porphyry copper type mineralization at Yeylagh-e-Gharechi deposit is developed within

quartz-monzonitic and monzonite bodies as disseminated, veins and veinlets. Porphyry mineralization is mainly developed within Gharechi quartz-monzonite as well as pyroclastics and volcanic.

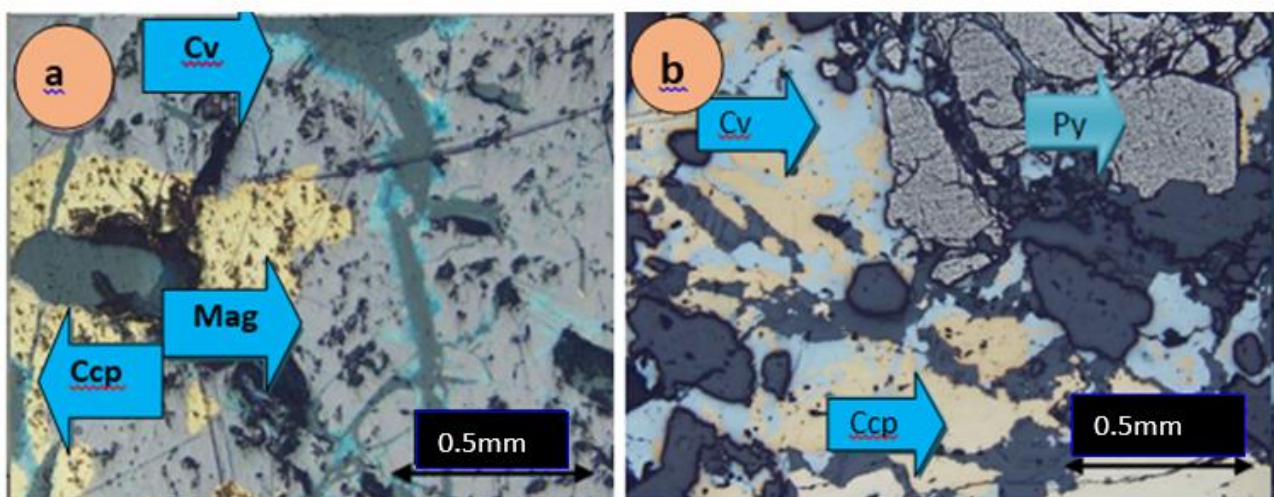


Fig 5a) Chalcopyrite (Ccp), Covellite (Cv) and Magnetite (Mag) in borehole No.1 at 165 depth. b) Covellite (Cv), Pyrite (Py) and Chalcopyrite (Ccp) in borehole No.2 at 149 depth.

Mineralization developed in hypogene zone. Hypogene mineralization developed during

potassic alteration. The process was especially intensified during potassic to phyllic transition.

Copper mineralization during potassic alteration was mainly as chalcopyrite and rare molybdenite. Mineralization is mainly as chalcopyrite developed during potassic alteration, while pyrite formed during potassic, phyllic and argillic alterations (Fig. 5).

Leached and supergene zone is eroded by erosion agents in Yeylagh-e-Gharechi area so the main parts of mineralization has demolished. Hypogene mineralization extend down to 480m based on the drilling, where average depth of hypogene zone is more than 200m. Sub surface

alteration zonation at Yeylagh-e-Gharechi deposit demonstrates conformity with Lowel-Guilbert porphyry system (Guilbert and Park, 1986) which was proposed in 1975. A little amount of quartz-sericite and siliceous alteration developed in this area. Supergene argillic alteration (Fig 6A) was observed associated with quartz vein and veinlets. Both hypogene and supergene alteration systems were developed at the study area. Potassic alteration (Fig 6B) developed mainly in porphyry quartz monzonite and monzonite stockwork in the central part of the system.

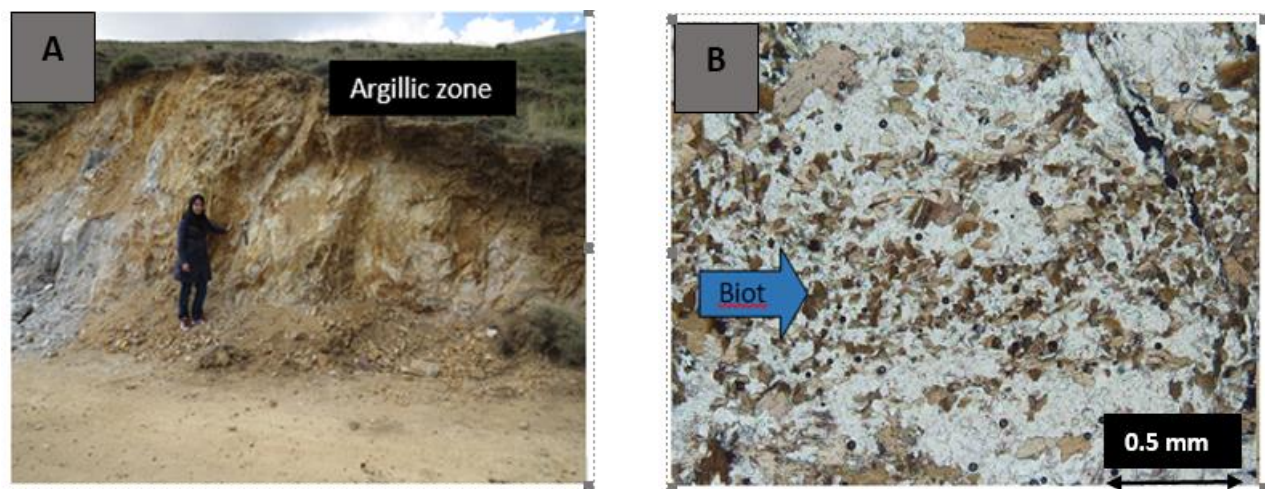


Figure 6A) Argillic zone in Yeylagh-e-Gharechi. B) newform biotite(Biot) in quartz monzonite in potassic alteration zone.

## 5- Classification of silica veinlets

Veins and veinlets developed at the Yeylagh-e-Gharechi deposit. Most of the veinlets consist of quartz, however, biotite, k-feldspar and sericitic veinlets are also observed. Quartz veinlets are mainly concentrated at both potassic and phyllic alteration, but potassic zone hosts more veinlets than phyllic zone. Four types of siliceous veinlets were recognized based on mineralogy and relative temporal relation:

I) The first type occurred mainly in potassic alteration halo, developed at the central and deeper parts of the porphyry system. They constitute of quartz + K-feldspar + biotite + pyrite + chalcopyrite  $\pm$  molybdenite (Fig. 7A).

Their irregular structure suggests that they were formed at a higher temperature, when they developed at a rather ductile condition, probably after porphyry stock crystallization. The width of the veinlets is generally less than 1 cm.

II) The second type cut across the first type or developed at the core of the first type veins during their re-opening (Fig. 7B). They consist of quartz + pyrite + chalcopyrite  $\pm$  anhydrite. Sulfide minerals developed at the center of the veins as thin discontinuous films. Sulfides are sometimes observed as disseminations within the veinlets. They are mainly observed at the potassic alteration zone, but are also rarely observed at the phyllic alteration zone. The

width of the veins are variable, but is generally less than 3 cm.

III) The third type which cut across the former types, consists of quartz + pyrite ± chalcopyrite. This type is concentrated at the argillic

alteration zone (Fig. 7C). The veinlets may exceed 5 cm in width.

IV) The last type which is composed of quartz, lack sulfide minerals and are observed at all alteration zones (Fig 7D).

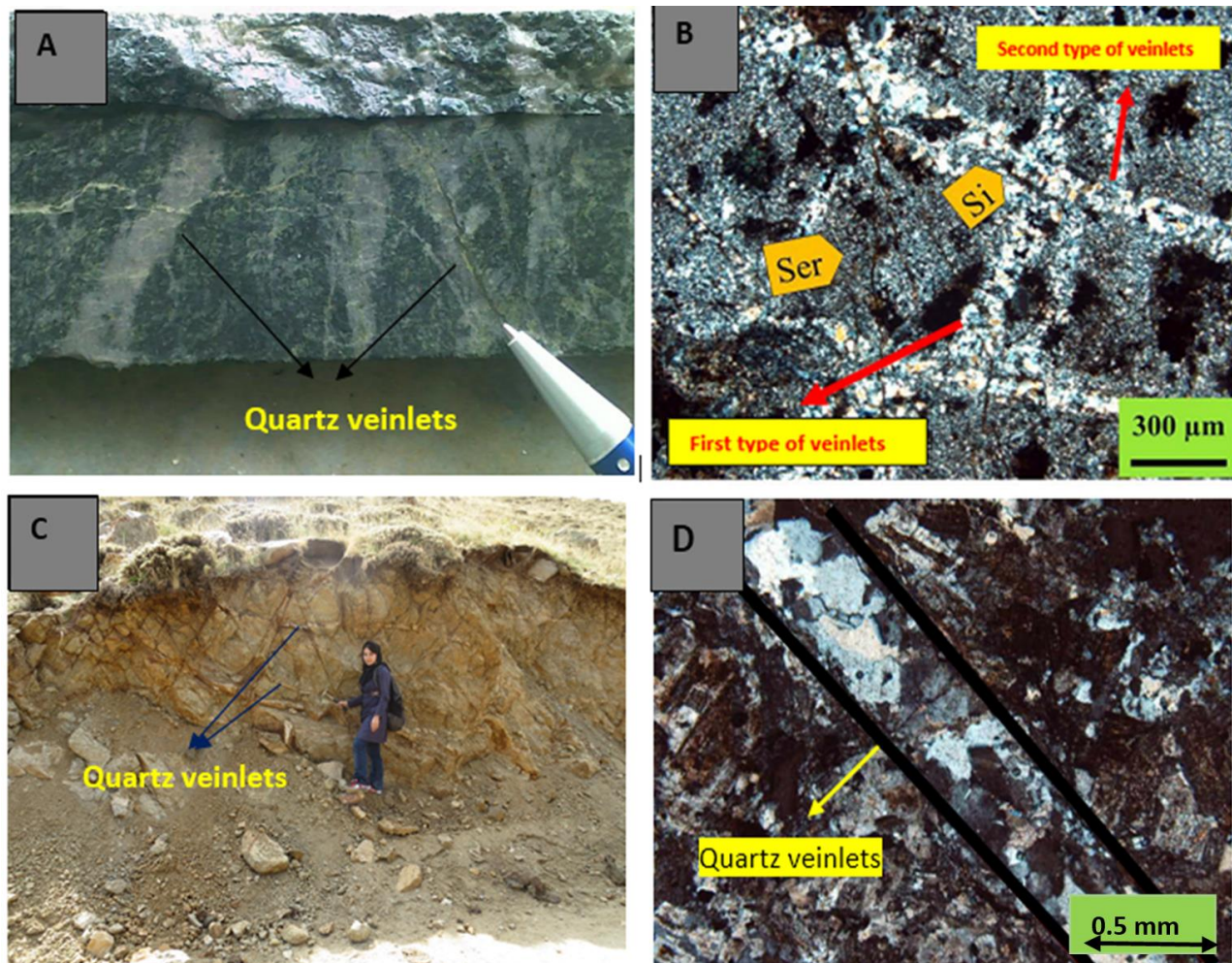


Figure 7A) The first type of quartz veinlets in potassic alteration zone. B) The second and first type of quartz veinlets in phyllic alteration zone. The second type across the first type veinlets. C) The third type of quartz veinlets that consist of quartz + pyrite + chalcopyrite. The width of veinlets is more than 5 cm. D) The last type of quartz veinlets in quartz diorite.

## 6- Methods

For this study, number of samples were collected from drill holes at Yeylagh-e-Gharechi deposit. About 138 thin section, 256 polished section and 6 double polished-thin section were prepared for petrography and fluid inclusion studies. The thin and polished section were examined under transmitted and reflected light at the Shahid beheshti university, Tehran, Iran. micro-thermometric studies were carried out on double polished-thin section.

Microthermometric measurements were made using linkam THMSG600 with combined heating and freezing stage with temperature range of -196 to +600 centigrade, attached to an Olympus petrographic microscope with PVTX software. The reproducibility of the measurements was better than  $\pm 0.1^{\circ}\text{C}$  for temperatures of less than +200 centigrade and  $\pm 1$  centigrade for temperatures between +200 to +600 centigrade. Stage calibration was carried out at  $45.6^{\circ}\text{C}$  (Chlorobenzene), and  $306/8^{\circ}\text{C}$  (Sodium-Nitrate) using standard synthetic fluid

inclusions. Ice-melting temperatures were determined at a heating rate of no more than 0.1°C/s. Homogenization temperatures were determined at a heating rate of 1°C/s. Homogenization of multi-phase solid inclusions was obtained with heating cycles of about 5°C. For two-phase inclusions, the homogenization temperature of liquid and vapor (predominant LV→L and rare LV→V) was recorded. In the multi-phase solid inclusions, two points were recorded: (1) Th (NaCl) (the temperature at which halite dissolved) and (2) Th (LV) (the temperature of vapour and liquid).

Several vein types from various depths were collected for laboratory analyses. Over 200 samples were investigated for the types of inclusion, their abundance, spatial distribution, and size. Eleven quartz wafers were polished at both sides using the procedure by Shepherd et al (1985). The thickness of the wafers varied between 100 and 150 µm, depending on the transparency of the quartz crystals. Fluid inclusion studies has done on quartz type I,II,III veinlets. Salinity determination of mineralizing fluids of inclusion was made using halite crystal solution temperature at the heating stage, PVTX Software Modelling and temperature to salinity conversion.

## 7- Fluid inclusion studies

Fluid inclusions are among unique indications which can decipher temperature, salinity, fluid chemical composition and the pressure governing the system due to their entrapment during millions of years (Bakker, 2011). Fluid inclusion studies can give us data on mineral forming temperature and mineralizing fluid chemical composition (Roedder, 1992).

### 7.1- Fluid inclusion petrography

Previous works on fluid inclusions of several porphyry deposits demonstrated complicated changes in fluid temperature and its composition in porphyry deposits both in time

and place (e.g. Eastoe, 1978; Preece and Beane 1982; Reynolds and Beane 1985). That's the case for the Yeylagh-e-Gharechi deposit. Fluid inclusion samples which were studied, collected from type I, II and III veinlets described above. The petrography characteristics of all types of veins are brought together. Most of the fluid inclusion sizes are not visible by naked eyes. The size of most fluid inclusions was generally between 1-10 µm, 10-100 µm sizes are rarely observed. The total volume of fluid inclusions on average were seldom more than 1% of the total host mineral volume (Roedder, 1992). Most of the fluid inclusions were as negative crystal or anhedral in shape, but spherical, bar-like, ovoidal, rectangular and irregular inclusions were also observed (Fig. 8).

Based on the petrographic studies, primary, secondary and pseudosecondary fluid inclusions were developed along microfractures, while their distribution within the crystal is random. The primary type of fluid inclusion are observed in I type vein lets (Potassic zone) and secondary and pseudosecondary type fluid inclusion are observed more common in the II and III types of veinlets (phyllic and argillic zone).

Petrographical and morphological characteristics of the fluid inclusions were recorded at room temperature by Roedder (1984) and Shepherd et al (1985). The discrimination of primary fluid inclusion were based on their single or random distribution within the crystal (Roedder, 1984).

In petrographical studies , there are four types of fluid inclusion according to internal phases:

*Single phase vapor-rich fluid inclusions (V):* most of the fluid inclusions at the Yeylagh-e-Gharechi deposit were of Single phase gaseous type which suggests probably boiling of mineralizing fluid and its gas-rich nature. These fluid inclusions observed were mainly smaller than 40 µm in size (Fig. 9). These types of fluid inclusion have observed in type I veinlets and to lesser extent in type II and type III veinlets.

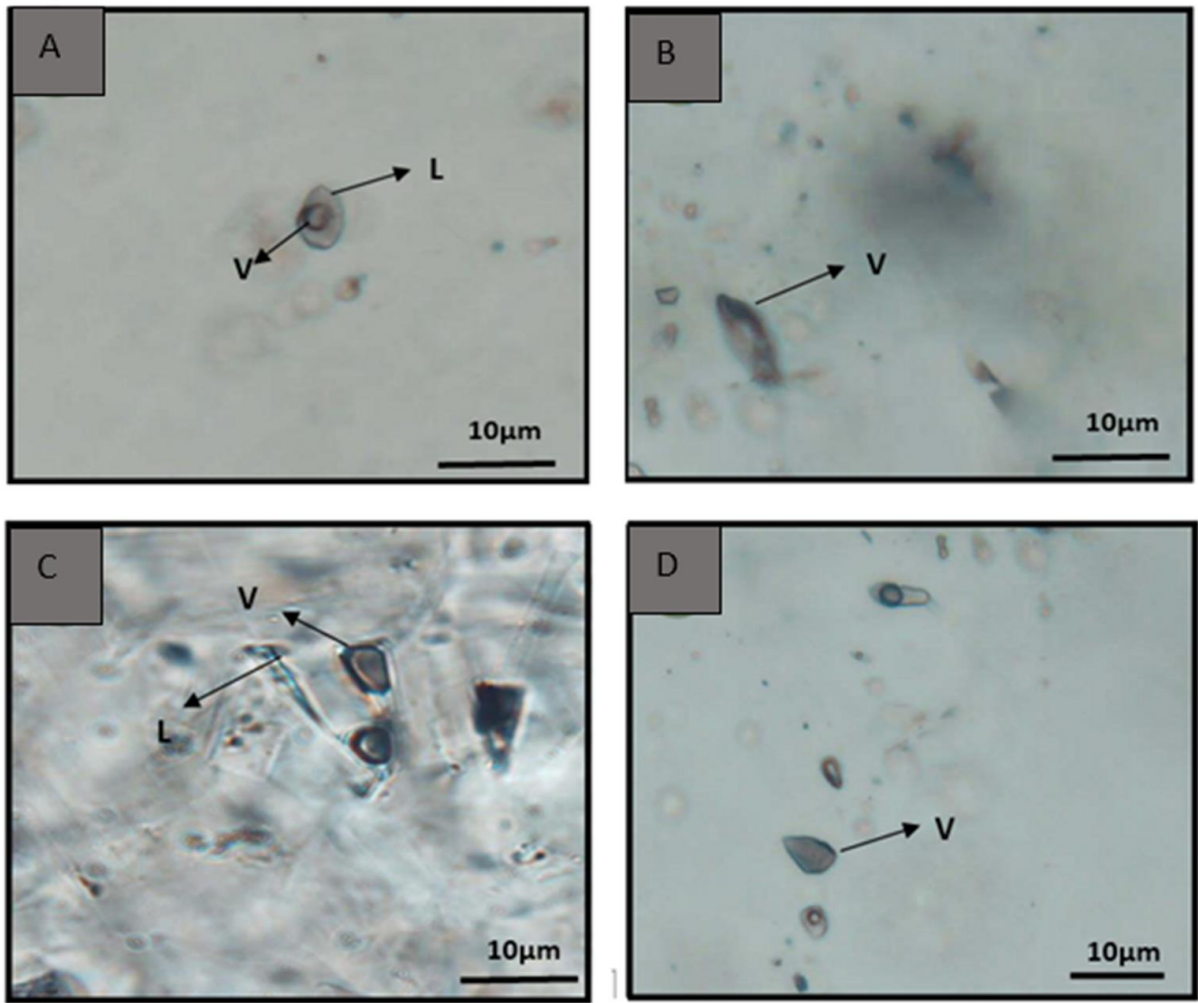


Figure 8A) Spherical from bore hole No.5, type II , B) Bar-like from bore hole No.2, type III, C) Treangular from bore hole No.6, type IV, D) Quartz negative crystal from bore hole No.5,type I. (V: vapor, L: liquid).

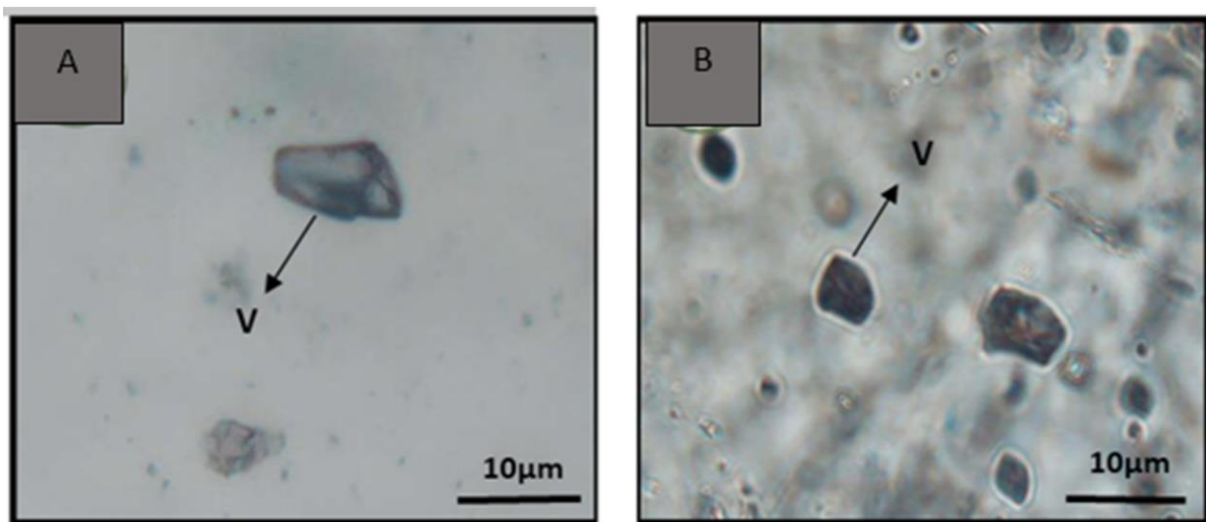


Figure 9) Gas rich fluid inclusions, A) borehole No.2, 153m, type I B) borehole No.3, 174m, type I, V:vapor

Liquid-rich fluid inclusions (L+V): these type of fluid inclusions were small in size and the most frequent fluid inclusions next to vapor-rich types. Their degree of filling (Df) was variable from 50-90%. The size of these liquid-rich

inclusions varied between 4-12 µm (Fig.10, A).These type of fluid inclusions are observed in type II of veinlets and in little amount in type I and type III of veinlets.

*Vapor-rich fluid inclusions (V+L):* Their size amounted to 15  $\mu\text{m}$  and distribution are irregular in quartz crystals. Sometimes they are

pseudo-secondary. Their degree of filling is less than 50%. These fluid inclusions are less frequency (Fig. 10B).

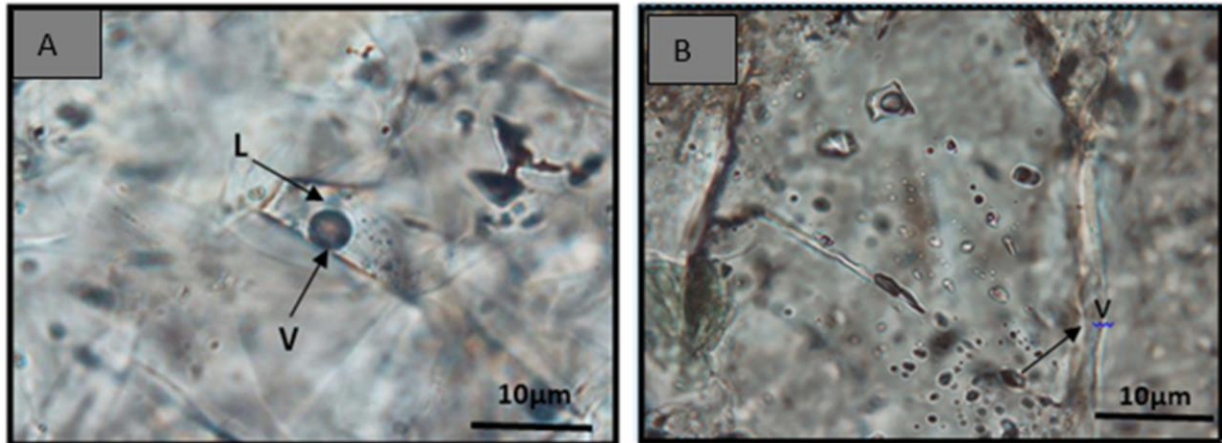


Figure 10A) Liquid-rich fluid inclusions, bore hole No.4, 98m, type II, B) Vapor-rich fluid inclusion, bore hole no.5, 55m, type III (V: vapor, L: liquid).

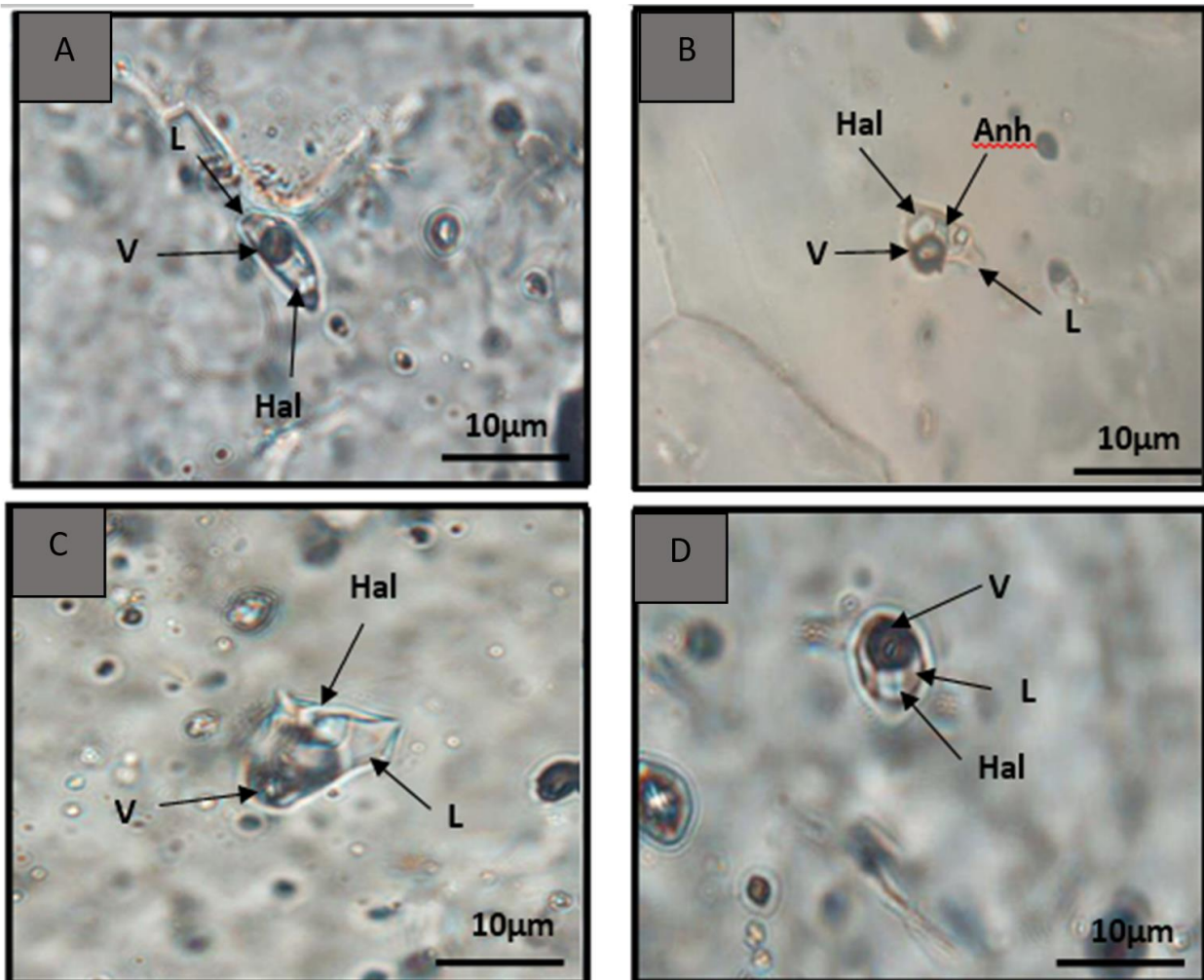


Figure 11) Solid-rich fluid inclusions A) bore hole No.4, 110 m, type I, B) bore hole NO 2, 185m, type I, C) bore hole No 2, 89 m, type II, .D) bore hole No 5, 73m, type II, V:vapor, L:liquid, Anh: anhydrite, Hal:halite

These types of fluid inclusions are observed mostly in type I of veinlets (potassic zone) and

in little amount in type II (phyllic zone) and type III (argillic zone) veinlets

**Solid-rich fluid inclusions (L+V+S):** These fluid inclusions were mainly observed where extensive potassic alteration occurred at the central part of the mineralization. These type of fluid inclusion are observed mostly in type I and type II but in type III and type IV are not observed. Daughter minerals observed in the

deposit were large halite crystals, smaller sylvite minerals, very small prismatic crystals of anhydrite with intermediate birefringence and red to black flaky hematite (Fig. 11). The identification of daughter phases within fluid is carried out only based on crystalline shape according to (Rodder, 1984).

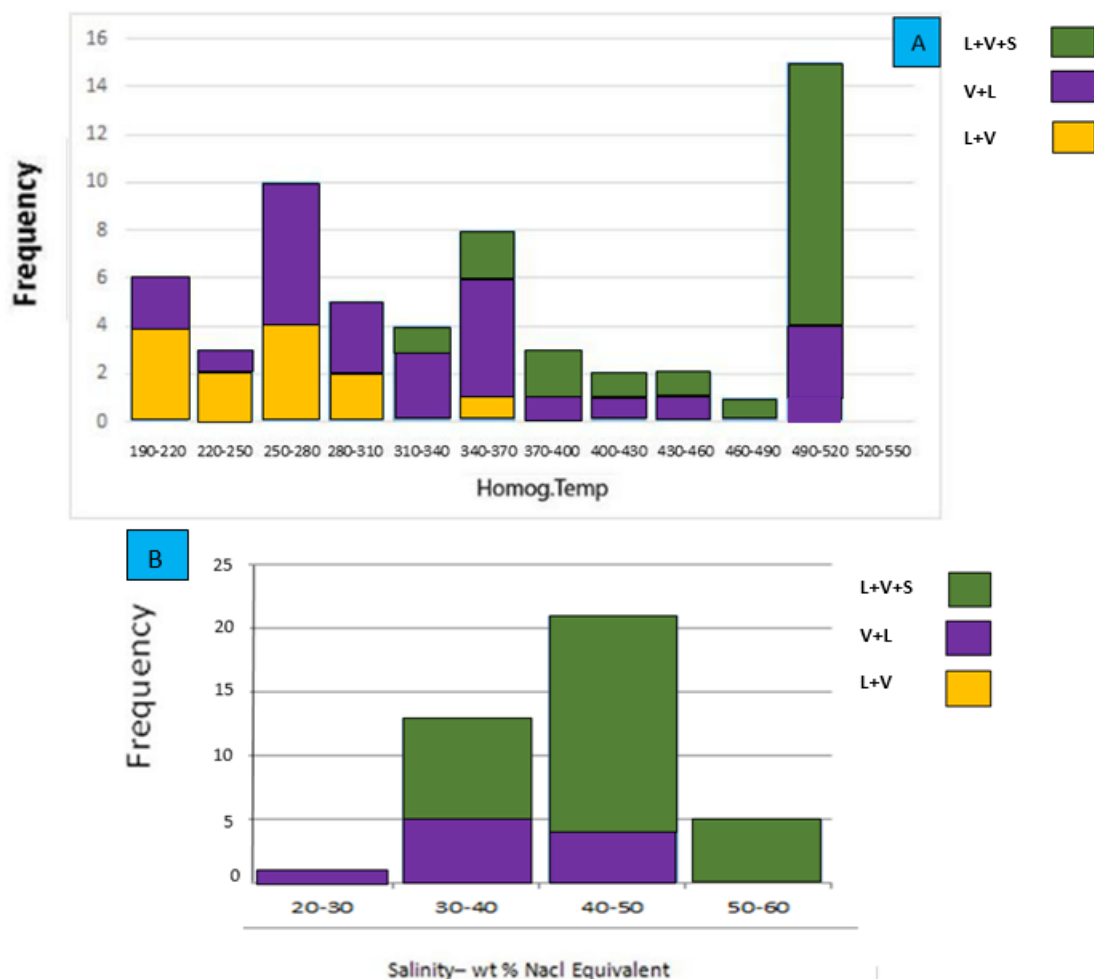


Figure 12A) Homogenization temperature versus frequency in samples from the study area B) salinity diagram versus frequency in samples from the study area

## 7.2- Fluid inclusion microthermometry

Thermometric analysis were done on primary large inclusions. Heating method was utilized for determination of homogenization temperature. Heating was applied to 59 fluid inclusions, the salinity of 40 fluid inclusions were also calculated (Hajalilou, 2017). We selected 33 sample from veinlets of type I ,17 sample from veinlets of type II and 9 sample veinlets of type III from total of 59 samples .Also we selected 19 samples from veinlets of

type I,13 samples from veinlets of II and 8 samples from III types from total of 40 samples.

The minimum salinity is recorded 20 with maximum 60 wt% NaCl equivalent. The homogenization temperature is between 190 to 520°C (Fig. 12). The results of salinity and homogenization temperature for each veinlets have been shown in (Fig. 12) by coloring.

Homogenization temperature in the studied fluid inclusions fall into three temperature ranges: low to medium temperature (250 to 280°C), medium temperature (340 to 370 °C) and high to

very high temperatures (490 to 520°C). The maximum homogenization temperature was recorded in saline fluid inclusions containing daughter halite±opaque minerals which often homogenized at disappearance of vapor phase into liquid phase. In some samples, salt solved into liquid phase. Halite solution temperature is higher than homogenization temperature and indicates entrapment in higher pressure (Bondar, 1994). Homogenization temperature of fluids which contained halite ±opaque occurred after dissolution of halite and generally recorded at 450 to 500°C. Multi-phase or halite-bearing fluid inclusions homogenization temperature occurred at vapor phase disappearance, were at medium and higher than 500°C temperatures. Two-phase fluid inclusions rich in liquid and two-phase fluid inclusions rich in vapor, were the smallest samples in number (11 inclusions of L+V types and 3 inclusions of V+L type).

Table 1) Homogenization temperature in quartz veinlets.

Phases	Type I	Type II	Type III
L+V	306-400 °C	263-318°C	195-271°C
V+L	426-495°C	385-417°C	-
V+L+S	495-520°C	490-496°C	-

Homogenization temperature of L+V was between 195 to 400°C. V+L homogenization temperature was between 385°C to 495°C. Most of the homogenization temperature frequencies in three-phase, was homogenization to liquid phase, with maximum temperature in the range of 490 to 520°C. Homogenization temperature of (L+V),(V+L) and (L+V+S) have been shown in related to quartz veinlets in table (1). Although halite daughter mineral was recognizable in most of the samples, the higher frequency of opaque daughter minerals especially hematite was considerable. Some samples had sylvite phase (triangular in shape) more than halite. Prevalent halite daughter minerals in fluid inclusions studied generally indicates higher Na and Cl content in magmatic-

hydrothermal fluids evolved in mineralizing system.

## 8- Discussion

Fluid inclusions at the Yeylagh-e-Gharechi deposit were mainly of gas-rich that occurred in type I quartz veinlets. However, multiphase fluid inclusions have also been widely observed. One phase vapor-rich types probably indicated fluid entrapment at boiling temperature, i.e. when vapor was in equilibrium with liquid (Roedder, 1992).

Parts of the copper content in the solution could be deposited as a result of boiling processes as chalcopyrite which was the major mineral at the Yeylagh-e-Gharechi deposit (similar to porphyry copper deposits).The evidences suggested that boiling had an important role in mineralization so that it looks there should be a temporal spatial relationship between fluid boiling and deposit formation (Samson, 2003). New physico-chemical conditions, changes in pH and temperature transitioning lithostatic to hydrostatic conditions associated with boiling led to quartz and sulfide deposition (Bodnar, 2014). Abundant stockwork and silica veins in the area associated with magnetite, molybdenite, quartz, pyrite and chalcopyrite as dissemination or vein-type is an evidence of the mineralization. Furthermore, saline fluid inclusions co-existing with vapor-rich fluid inclusions indicate high temperature of boiling .

Fluid inclusions results on the samples taken from the study area were plotted on a diagram where homogenization temperature versus salinity of typical porphyry, skarn and epithermal deposits were also plotted (Fig. 16). The diagram demonstrates that the final homogenization temperature and salinity of the fluid inclusions fall in the range of fluid inclusions which are typical for porphyry deposits (Wilkinson, 2011). Magmatic-hydrothermal fluid evolution tends toward lower

temperature-salinity resulting from mixing with meteoric water at a later stages.

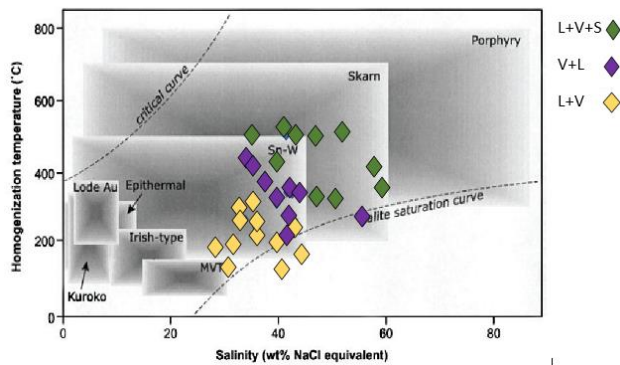


Figure 16) Salinity versus final homogenization temperature the Yeylagh-e-Gharechi deposit within the range of common fluid inclusions of the deposits (based on Wilkinson, 2011).

Fluid inclusion studies demonstrates a decrease in temperature and salinity of the fluids from potassic alteration to argillic alteration.

Salinity versus homogenization temperature diagram was utilized for determination of source of the mineralizing fluids (Wilkinson, 2001). Plotting the data on the diagram (Fig. 17) demonstrates that the mineralization at the Yeylagh-e-Gharechi porphyry copper deposit was related to fluids of magmatic-saline and sea water origin. It can be deduced that the majority of the waters involved in potassic alteration were of magmatic and sea water source. In other words, solutions of magmatic origin were active only at the central core of the mineralization (Takenouchi, 2001).

Density variation is very important in recognition of fluid flow mechanism and its spatial change in a hydrothermal system (Wilkinson, 2001). Density variation at the Yeylagh-e-Gharechi deposit versus temperature and salinity indicates increasing density with decreasing temperature and increasing salinity. Densities up to 1.2 gr/cm<sup>3</sup> and close to 1.3 were also observed which suggests mineralizing fluids rich in solid phases (Fig. 18).

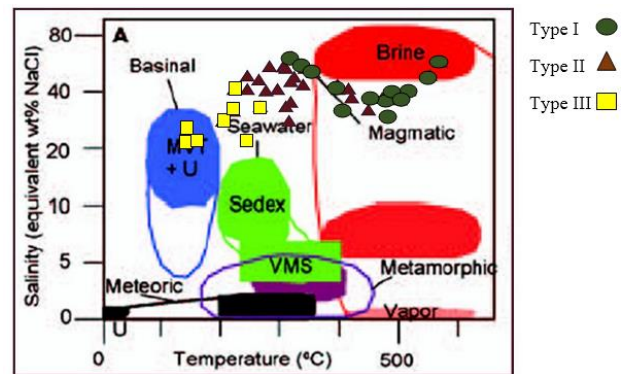


Figure 17) Homogenization temperature versus salinity of fluid inclusions of the study area (Wilkinson, 2001).

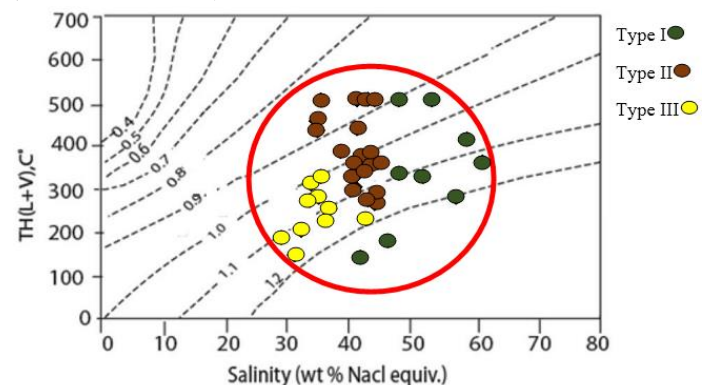


Figure 18) Density variation versus temperature and salinity where the density of NaCl solutions saturated in vapor were plotted (Wilkinson, 2001).

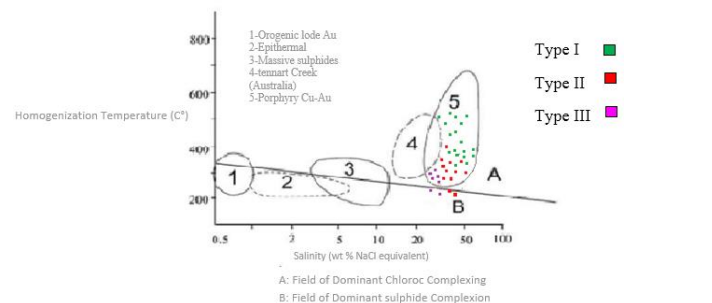


Figure 19) Homogenization temperature versus salinity of fluid inclusions within hydrothermal mineralization systems (Large, 1998).

The results obtained from fluid inclusion salinity and homogenization temperature studies were plotted on homogenization temperature versus salinity diagram of hydrothermal mineralization systems (Large, 1998; Fig. 19). The diagram had five distinct area which were 1-Archaen orogenic gold 2- epithermal gold-silver 3- volcanogenic massive sulfide 4- Australian Tenent Creek Cu-Au deposits and 5- porphyry Cu-Au deposits. Part A demonstrates metal transport as chloride complexes whereas

part B indicates metal transport as bisulfide complexes. As it was illustrated in the diagram, all the samples from located at the fifth district which represents porphyry Cu-Au deposits where the dominant transport for metal was as chloride complexes.

## 9- Conclusion

The Yeylagh-e-Gharechi porphyry copper deposit is located in Arasbaran metallogenic belt and northwest of Iran. Quartz monzonitic and monzodioritic stock is the most important agent for copper mineralization. According to studies the variety of quartz have recognized. Based on the internal phases, there are four types of fluid inclusion which includes gas-rich phase, liquid-rich phase, two phases liquid-rich, two phase vapor-rich and multiphase solid-rich ones. Homogenization temperature of fluid inclusions at the Yeylagh-e-Gharechi porphyry copper deposit ranged between 190 to 520°C and the salinity between 20-60 wt % NaCl equivalents. The fluid inclusion studies followed decreasing in homogenization temperature and salinity from potassic alteration to argillic alteration. The maximum homogenization temperature of 520°C recorded in potassic alteration zone while the minimum temperature of 190°C recorded in argillic alteration zone. Based on the fluid inclusion studies it can be proposed that probably Yeylagh-e-Gharechi is a copper type porphyry deposit.

## Acknowledgement

Thanks the Mehr Asl Company for provide sampling from the deposit and boreholes cores.

## References

- Aghanabati, A. 2006. The Geology of Iran, Geological Survey of Iran, 708 p.
- Aghazadeh, M., Hou, Z., Badrzadeh, Z., Zhou, L. 2015. Temporal-Spatial Distribution and Tectonic Setting of Porphyry Copper Deposits in Iran: Constraints from Zircon U-Pb and Molybdenite Re-Os Geochronology. *Ore Geology Reviews*: 70, 385–406.
- Aghazadeh, M., Castro, A., Omran, N. R., Emami, M. H., Moinvaziri, H., Badrzadeh, Z. 2010. The Gabbro (Shoshonitic)-Monzonite-Granodiorite Association of Khankandi Pluton, Alborz Mountains, NW Iran. *Journal of Asian Earth Sciences*: 38, 199–219.
- Aghazadeh, M., Castro, A., Badrzadeh, Z., Vogt, K. 2011. Post-Collisional Polycyclic Plutonism from the Zagros Hinterland: The Sheivar Dagh Plutonic Complex, Alborz Belt, Iran. *Geological Magazine*, 148, 980–1008.
- Babakhani, A. R., Lesquyer, J. L., Rico, R. 1990. Geological Map of Ahar Quadrangle (Scale 1:250,000). Geological Survey of Iran, Tehran, Iran.
- Bakker, R. J. 2011. Fluid Inclusions; Critical Review, Applications, Computer Modeling. Short Course. University of Leoben, Leoben.
- Beane, R. E., Bodnar, R. J. 1995. Hydrothermal Fluids and Hydrothermal Alteration in Porphyry Copper Deposits. In: Pierce, F. W. and Bohm, J. G., Eds., *Porphyry Copper Deposits of the American Cordillera*, Arizona Geological Society Digest: 20, Tucson, 83–93.
- Bodnar, R. J. 1994. Synthetic Fluid Inclusions: XII. The System H<sub>2</sub>O-NaCl. Experimental Determination of the Halite Liquidus and Isochores for a 40 wt% NaCl Solution. *Geochimica et Cosmochimica Acta*: 58, 1053–1063.
- Castro, A., Aghazadeh, M., Badrzadeh, Z., Chichorro, M. 2013. Late Eocene-Oligocene Post-Collisional Monzonitic Intrusions from the Alborz Magmatic Belt, NW Iran. An Example of Monzonite

- Magma Generation from a Metasomatized Mantle Source. *Lithos*: 180-181, 109–127.
- Cooke, D. R., Hollings, P., Walsh, J. L. 2005 Giant Porphyry Deposit Characteristics, Distribution, and Tectonic Controls. *Economic geology*: 100, 801–818.
- Eastoe, C. J. 1978. A Fluid Inclusion Study of the Panguna Porphyry Copper Deposit, Bougainville, Papua New Guinea. *Economic-Geology*: 73, 721–748.
- Guilbert, J. M., Park, C. F. 1986. *The Geology of Ore Deposits*. W. H. Freeman and Company, New York.
- Gustafson, L. B., Hunt, J. P. 1975. The Porphyry Copper Deposit at El Salvador, Chile. *Economic Geology*: 70, 857–912.
- Hajalilou, B. 2011. *Fluid Inclusion Geothermometry*. Payame Noor University Press, Tehran (In Persian).
- Hajalilou, B. 2012. Final Report of Exploration in Ali Javad Area. Ministry of Industry, Mine and Trading, Mehr Asl Company (In Persian).
- Hajalilou, B., Aghazadeh, M. 2016. Fluid Inclusion Studies on Quartz Veinlets at the Ali Javad Porphyry Copper (Gold) Deposit, Arasbaran, Northwestern Iran, *Journal of Geoscience and Environment Protection*: 4, 80–91.
- Hajalilou, N. 2017. Economic geology investigation of copper mineralization in south west of Sheivar Dagh, North of Ahar, East Azerbaijan. MSc thesis at Geoscience faculty in Shahid Beheshti University, 206 pp.
- Jahangiri, A. 2007. Post-Collisional Miocene Adakitic Volcanism in NW Iran: Geochemical and Geodynamic Implications. *Journal of Asia Earth Sciences*: 30, 433–47.
- Jamali, H., Dilek, Y., Daliran, F., Yaghubpur, A., Mehrabi, B. 2009. Metallogeny and Tectonic Evolution of the Cenozoic Ahar-Arasbaran Volcanic Belt, Northern Iran. *International Geology Reviews*: 52, 608–630.
- Large, R. R., Bull, S. W., Cooke, D. R., McGoldrick, P. J. 1998. A Genetic Model for the HYC Deposit, Australia, Based on Regional Sedimentology, Geochemistry and Sulfide-Sediment Relationship. *Economic Geology*: 93, 1345–1368.
- Mehrpour, M. 1993. Contributions to the Geology, Geochemistry, Ore Genesis and Fluid Inclusion Investigations on Sungun Cu-Mo Porphyry Deposit (North- West of Iran). Ph.D. Thesis, Hamburg University, Hamburg, Germany.
- Moritz, R., Rezeau, H., Ovtcharova, H., Tayan, R., Melkonyan, R., Hovakimyan, S., Ramazanov, V., Selby, D., Ulianov, A., Chiaradia, M., Putlitz, B. 2016. Long-Lived, Stationary Magmatism and Pulsed Porphyry Systems during Tethyan Subduction to Post-Collision Evolution in the Southernmost Lesser Caucasus, Armenia and Nakhitchevan. *Gondwana Research*: 37, 465–503.
- Preece, R. K., Bean, R. E. 1982. Contrasting Evolutions of Hydrothermal Alteration in Quartz Monzonite and Quartz Diorite Wall Rocks at the Sierrita Porphyry Copper Deposit, Arizona. *Economic Geology*, 77, 1621–1641.
- Reynolds, T. J., Bean, R. E. 1985. Evolution of Hydrothermal Fluid Characteristics at the Santa Rita, New Mexico, Porphyry Copper Deposit. *Economic Geology*: 80, 1328–1347.
- Roedder, E. 1992. Fluid Inclusion Evidence for Immiscibility in Magmatic Differentiation. *Geochimica et Cosmochimica Acta*: 56, 5–20.
- Samson, I., Anderson, A., Marshall, D. D. 2003. *Fluid Inclusions: Analysis and Interpretation*. Mineralogical Association of Canada.

- Seedorf, E., Dilles, J. H., Proffett, J. M., Einaudi, M. T., Zurcher, L., Stavast, W. J. A., Johnson, D. A., Barton, M. D. 2005. Porphyry Deposits: Characteristics and Origin of Hypogene Features. *Economic Geology* (100th Anniversary): 251–298.
- Shafiei, B., Haschke, M., Shahabpour, J. 2009. Recycling of Orogenic Arc Crust Triggers Porphyry Cu Mineralization in Kerman Cenozoic Arc Rocks, Southeastern Iran. *Mineralium Deposita*: 44, 265–283.
- Shepherd, T. J., Rankin, A. H., Alderton, D. H. M. 1985. *A Practical Guide to Fluid Inclusion Studies*. Blackie Press, London.
- Sillitoe, R. H. 2010. Porphyry Copper Systems. *Economic Geology*: 105, 3–41.
- Takenouchi, S. 1980. Preliminary Studies on Fluid Inclusions of the Santo Tomas II (Philex) and Tapian (Marcroper) Porphyry Copper Deposits in the Philippines. *Mining Geology* (Special Issue): 8, 141–150.
- Wilkinson, J. J. 2011. Fluid Inclusions in Hydrothermal Ore Deposits. *Lithos*: 55, 229–272.